Improvement of SRK Equation of State for Vapor-Liquid Equilibria of Petroleum Fluids

Li-Sheng Wang
Dept. of Chemical Engineering, Beijing Institute of Technology, 100081 People's Republic of China

Jürgen Gmehling
Universität Oldenburg, Technische Chemie, D-26111 Oldenburg, Germany

To improve the SRK equation of state for the calculation of vapor-liquid equilibria of petroleum fluids, the parameters of the Mathias-Copeman α-function were refitted to a large number of experimental vapor-pressure data (15,311 data points) stored in the Dortmund Data Bank with a particular view to improving the accuracy of the vapor-pressure correlation in the low pressure range. Using the new parameters, vapor-liquid equilibria were calculated using two different mixing rules: the group contribution mixing rule for the mixture parameters a of the SRK EOS; the conventional mixing rules for the mixture parameters a and b of the SRK EOS together with a characterization method developed on the basis of existing empirical correlations for the properties of plus fractions of undefined mixtures. The results show that the accuracy for crude oil and natural gas mixtures can be improved by refitting the SRK EOS parameters.

Introduction

Simple cubic equations-of-state (EOS) of the van der Waals type are often preferred due to their potential for achieving the desired compromises. The most popular cubic EOSs are based on the RK equation (Redlich and Kwong, 1949) and its modifications. The RK EOS as modified by Soave (1972) (SRK) is widely used for representing vapor-liquid equilibrium (VLE) data.

In order to improve the performance of the SRK EOS for satisfying the requirements of VLE calculations, Mathias and Copeman (1983) proposed an α-function which is a polynomial extension of the original Soave α-function which can significantly improve the accuracy for vapor pressures at low pressures.

The development of reliable methods for the calculation of phase equilibria requires the necessary parameters to be fitted using a large database covering a wide temperature and pressure range. The Dortmund Data Bank (DDB), which started in 1973 in Dortmund and since 1989 further developed in Oldenburg, represents the largest computerized data bank for thermodynamic pure component and mixture properties. Today, the DDB contains more than 110,000 vapor-pressure data.

Up to now, the most important success of the SRK EOS is its wide application in the oil and gas production and processing industry (Pedersen et al., 1984). However, the prediction of VLE for undefined petroleum mixtures is usually not satisfactory. In order to improve the SRK EOS, this study mainly concerns components of petroleum fluids, such as CO_2, N_2, H_2O (important ternary oil recovery fluids), H_2S (an important component of sour natural gases), methanol (gas hydrate inhibiting agent in natural gas production), as well as paraffins, naphthenes, and aromatics (PNA). First of all, the required Mathias-Copeman parameters were fitted to a large number of experimental vapor-pressure data for these petroleum fluids. A characterization method is proposed for the SRK equation of state on the basis of existing empirical correlations for the properties of plus fractions of petroleum and natural gas mixtures. Some analytical data including composition analysis, molecular weights, and densities of plus fractions and phase equilibrium data for various reservoir crude oils and natural gases have been collected. These different phase equilibrium data were calculated and compared

Correspondence concerning this article should be addressed to J. Gmehling.

by using the new fitted model and the original SRK model (Soave, 1972) in order to demonstrate the advantage of fitting EOS parameters to a large database.

SRK EOS and Calculation Results for Saturated Vapor Pressure

The original SRK EOS is (Soave, 1972)

$$P = \frac{RT}{v - b} - \frac{a(T)}{v(v + b)} \tag{1}$$

For pure components, the energy parameter $a(T)$ can be calculated from

$$a(T) = a\alpha(T_r) \tag{2}$$

whereby the parameters a and b are expressed as

$$a = 0.42748 \frac{R^2 T_c^2}{P_c} \tag{3}$$

$$b = 0.08664 \frac{RT_c}{P_c} \tag{4}$$

The α-function given in Eq. 2 is calculated according to the Mathias-Copeman expression, which is able to describe the temperature dependence of $a(T)$ more accurately at low pressures (Mathias and Copeman, 1983)

$$a(T_r) = \left[1 + m_1\left(1 - \sqrt{T_r}\right) + m_2\left(1 - \sqrt{T_r}\right)^2 + m_3\left(1 - \sqrt{T_r}\right)^3\right]^2 \quad \text{for } T_r \le 1 \tag{5}$$

$$a(T_r) = \left[1 + m_1\left(1 - \sqrt{T_r}\right)\right]^2 \quad \text{for } T_r > 1 \tag{6}$$

In this work, a large number of experimental vapor-pressure data stored in the Dortmund Data Bank (DDB) were fitted to obtain the required parameters m_1, m_2, and m_3. The results are listed in Table 1 together with the critical temperatures, critical pressures, and acentric factors used. Initially, the calculations were performed by fitting a generalized function for m_1 for all substances. In this case, the results obtained are given in the column SRK-1. The calculated results for all substances listed in Table 1 are based on the following generalized expression (G) as a function of the acentric factor ω

$$m_1 = 0.48344 + 1.58597\omega - 0.3758\omega^2 + 0.23194\omega^3 \tag{7}$$

Slightly better results are obtained when compared with the results based on the original generalized expression of m_1 given by Soave (1972). The average relative deviations between experimental and calculated vapor-pressure data (in total 15,311 data points) were reduced from 3.66% to 3.53%.

After having established the generalized parameter m_1, the experimental data were used to fit the parameters m_2 and m_3 in order to improve the results. The deviations obtained using three terms (Eq. 5) are also listed in Table 1 (column SRK-2). It can be seen that the average deviation is reduced to 1.96%. Figure 1 shows the fitted results of SRK-2 for toluene as an example. It can be seen that if a large number of data points are fitted, the error of scattering experimental data is compensated. For most of the substances, only parameter m_2 had to be fitted to improve the results significantly as shown in Table 1. However, for a few substances such as water, good results are only obtained when not only m_2 but also m_3 is used. The parameters m_2 and m_3 are specific for each component. However, for alkanes from *n*-heptane to eicosane following generalized expressions were developed for m_2 depending on the value of the acentric factor ω

$$m_2 = 0 \qquad (0.35 < \omega \le 0.56) \tag{8}$$

$$m_2 = 25.689 - 108.63\omega + 150.68\omega^2 - 68.739\omega^3 \quad (\omega > 0.56) \tag{9}$$

The generalized and revised SRK equation of state can be applied even for complex petroleum fluids. Components such as CO_2, N_2, C_1, C_2, C_3, iC_4, nC_4, iC_5, nC_5, and nC_6 are treated as defined components, so that there is no problem in using specific parameters for these components. The undefined heavy cuts are usually expressed in C_7^+ fractions. In this case, Eqs. 8 and 9 can be used.

Besides the comparison between the original SRK equation of state and the SRK-1 model, a comparison with the results obtained using the equations of state proposed by Peng and Robinson (1976), Yu and Lu (1987), and Schmidt and Wenzel (1980) is additionally given in Table 1. The overall average relative vapor-pressure deviations given by these equations of state are 5.28% (Peng and Robinson), 4.19% (Yu and Lu) and 3.58% (Schmidt and Wenzel), respectively. Significant improvement has been obtained by the proposed SRK-2 model, where the overall average relative deviation is 1.96%. For the substances calculated by both SRK-1 and SRK-2 models, the values of the parameters m_1 and m_2 are replaced by "G" in Table 1, when the generalized parameters are used.

Extension to Binary Mixtures

The PSRK (Predictive SRK EOS) group contribution mixing rule for the mixture parameters a and b is employed in this work to carry out all the calculations. The PSRK model combines the UNIFAC model with the SRK EOS. The PSRK yields satisfactory VLE predictions for systems containing not only nonpolar, but also polar components and asymmetric systems (Holderbaum and Gmehling, 1991; Fischer and Gmehling, 1996; Gmehling et al., 1997; Li et al., 1998)

$$\frac{a}{bRT} = \frac{1}{A_0}\left(\sum x_i \ln \gamma_i + \sum x_i \ln \frac{b}{b_i}\right) + \sum x_i \frac{a_i}{b_i RT} \tag{10}$$

where

$$A_0 = -0.64663 \tag{11}$$

$$b = \sum x_i b_i \tag{12}$$

Table 1. Calculated Saturated Vapor Pressure of 54 Substances Based on Different Equations of State vs. Experimental Data in the Dortmund Data Bank

Component	Data Points	T Range (K)	P Range (kPa)	Tc (K)	Pc (atm)	ω	m_1	m_2	m_3	AAPD% SRK-1	SRK-2	SRK	PR	YL	SW
Methanol	1,135	174.04–512.58	0.1693–8,097.000	512.6	79.90	0.5590	1.4371	-7.9942×10^{-1}	0.3278	*	1.12	*	*	6.50	*
Carbon dioxide	277	163.41–304.10	4.7600–7,369.000	304.2	72.80	0.2250	G	−1.9446	15.2851	14.29	1.42	14.40	14.63	15.72	15.00
Nitrogen	210	63.14–126.15	12.5200–3,391.000	126.2	33.50	0.0400	G	-5.4127×10^{-2}	0	1.72	1.03	1.48	0.86	1.69	1.25
Hydrogen sulfide	116	187.66–370.00	23.1600–8,501.000	373.2	88.20	0.1000	G	-3.6204×10^{-2}	0	1.72	0.96	1.36	1.46	2.23	1.35
Methane	407	89.80–190.53	10.7800–4,596.000	190.6	45.40	0.0080	G	-5.9041×10^{-2}	0	2.49	1.44	2.15	1.61	1.66	0.98
Cyclopentane	122	213.91–503.21	0.3130–4,023.000	511.7	44.51	0.1920	G	5.7868×10^{-3}	0	0.79	0.57	1.28	4.16	3.17	2.18
Cyclohexane	979	267.80–552.60	2.6600–4,023.000	553.8	40.27	0.2130	G	0	0	1.15	1.15	0.93	2.53	2.17	1.31
Cycloheptane	75	283.05–599.40	1.2720–3,661.000	604.2	37.70	0.2360	G	2.2121×10^{-2}	0	1.43	0.50	1.53	3.02	2.72	2.17
Cyclooctane	110	288.15–641.60	0.4030–3,410.000	647.2	35.13	0.2510	G	6.9743×10^{-3}	0	3.45	1.59	3.46	5.91	5.18	4.24
Benzene	1,846	260.15–561.65	1.3450–4,849.000	562.1	48.30	0.2120	G	0	0	0.92	0.92	0.97	3.19	2.69	1.81
Toluene	859	263.45–591.27	0.4706–4,093.000	591.7	40.60	0.2570	G	2.7551×10^{-2}	0	2.73	1.53	2.69	4.83	4.02	3.31
Ethylbenzene	305	273.16–611.10	0.2560–3,342.000	617.1	35.60	0.3010	G	1.9083×10^{-2}	0	2.14	1.80	1.79	4.13	2.51	1.96
Propylbenzene	79	313.15–433.39	1.0990–104.000	638.3	31.60	0.3440	G	-4.9818×10^{-3}	0	4.54	4.49	5.13	5.19	4.44	4.46
Butylbenzene	73	312.94–457.48	0.4050–104.000	660.5	28.50	0.3920	G	0	0	1.46	1.46	2.33	1.24	2.11	1.46
Hexylbenzene	12	353.58–462.97	0.5891–40.690	695.4	25.21	0.5290	G	-1.2950×10^{-1}	0	8.97	1.64	10.85	6.30	13.63	11.19
Octylbenzene	12	373.22–462.87	0.3620–14.270	728.0	20.10	0.5883	G	-7.5181×10^{-2}	0	6.29	2.66	8.15	2.58	10.37	9.41
p-Xylene	297	283.15–611.15	0.3066–3,314.000	616.2	34.70	0.3240	G	-1.1010×10^{-1}	0.2986	3.28	2.72	3.66	2.83	2.61	2.81
m-Xylene	223	283.15–616.71	0.2933–3,521.000	617.0	35.00	0.3310	G	-4.0179×10^{-2}	0	3.38	2.08	3.82	2.05	2.90	2.86
o-Xylene	190	283.15–625.15	0.2133–3,519.000	630.2	36.80	0.3140	G	-2.8656×10^{-2}	0	3.49	2.49	3.84	2.53	2.70	2.50
Naphthalene	520	334.95–740.15	0.3013–3,619.000	748.4	40.00	0.3020	G	-2.9986×10^{-3}	0	1.22	1.21	1.32	2.14	1.16	1.12
1-Methyl naphthalene	111	353.64–755.37	0.3565–3,027.000	772.0	35.20	0.3340	G	6.2326×10^{-2}	0	4.01	1.12	3.33	5.09	4.00	3.97
1-Ethyl naphthalene	13	393.15–531.45	1.3330–101.300	775.6	30.60	0.3767	G	9.0196×10^{-2}	0	7.35	0.95	6.07	9.38	6.39	7.68
Ethane	355	113.40–305.32	0.1333–4,873.000	305.4	48.20	0.0980	G	-4.4576×10^{-2}	0	2.54	1.86	2.24	2.03	2.02	1.33
Propane	557	144.26–369.65	0.1290–4,232.000	369.8	41.90	0.1520	G	-3.6204×10^{-2}	0	2.66	2.20	2.49	2.39	2.63	1.99
i-Butane	222	166.90–408.14	0.4000–3,648.000	408.8	35.92	0.1760	G	0	0	2.83	2.17	2.74	3.24	4.22	3.30
n-Butane	329	177.59–424.86	0.2410–3,760.000	425.2	37.50	0.1930	G	1.5292×10^{-2}	0	2.18	1.91	2.41	3.01	2.41	2.04
i-Pentane	150	193.62–453.15	0.1920–3,013.000	460.4	33.36	0.2270	G	0	0	1.94	1.96	1.86	2.40	1.54	1.47
n-Pentane	322	207.97–461.35	0.4106–2,959.000	469.7	33.25	0.2510	G	-1.3734×10^{-2}	0	1.05	0.88	1.05	0.72	0.76	0.48
n-Hexane	937	228.15–503.15	0.3106–2,794.000	507.4	29.75	0.2960	G	1.8354×10^{-2}	0	1.77	1.18	1.46	2.64	2.24	2.04
n-Heptane	714	258.15–540.00	0.5520–2,736.000	540.3	26.98	0.3510	G	G	0	1.00	1.00	1.56	1.18	1.03	0.75
n-Octane	409	269.85–563.15	0.3000–2,298.000	568.8	24.62	0.3940	G	G	0	2.97	2.82	1.87	3.92	1.35	2.80
n-Nonane	95	293.15–424.94	0.3910–104.000	594.7	22.50	0.4440	G	G	0	2.01	1.87	1.79	2.67	3.02	1.64
n-Decane	248	303.15–588.13	0.2533–1,395.000	617.9	20.72	0.4900	G	G	0	2.71	2.60	2.99	3.59	5.69	3.63
Undecane	29	333.15–470.42	0.5506–104.800	638.4	19.23	0.5350	G	G	0	2.13	1.95	1.37	3.26	3.24	1.35
Dodecane	131	333.15–651.15	0.2266–1,539.000	658.8	17.86	0.5620	G	G	0	3.69	2.54	2.59	7.09	1.92	2.18
Tridecane	29	377.15–509.21	1.3330–102.800	676.0	16.57	0.6230	G	G	0	4.42	2.04	5.32	2.45	6.51	5.83
Tetradecane	71	373.08–588.13	0.4429–343.400	691.8	15.52	0.6790	G	G	0	4.84	1.44	4.95	2.11	6.31	6.40
Pentadecane	20	384.15–543.65	0.3840–101.100	707.0	14.60	0.7060	G	G	0	3.75	2.03	3.57	2.42	4.80	5.23
Hexadecane	73	393.05–589.00	0.3176–188.000	722.4	13.83	0.7420	G	G	0	4.72	3.38	3.86	3.15	5.54	6.45
Heptadecane	11	333.15–434.05	0.0015–1.373	735.9	13.24	0.7700	G	G	0	10.89	4.62	13.57	51.60	5.06	5.87
Octadecane	22	413.07–590.65	0.2640–100.000	747.7	12.75	0.7900	G	G	0	5.28	4.16	8.11	20.93	6.04	3.85
Nonadecane	17	423.04–588.13	0.2550–73.660	756.0	11.00	0.8270	G	G	0	1.64	1.34	5.86	18.93	4.76	1.81
Eicosane	63	439.50–625.99	0.2818–120.800	767.0	11.00	0.9070	G	G	0	7.51	2.88	3.14	13.17	3.19	7.62
Ethylene	303	101.53–282.30	0.0757–5,036.000	282.4	49.70	0.0850	G	0	0	4.75	1.86	4.59	9.93	9.10	5.70
Propylene	281	145.02–364.55	0.2280–4,600.000	365.0	45.60	0.1480	G	-4.4018×10^{-2}	0	2.32	1.44	2.07	1.76	2.38	1.86
1-Butene	139	195.65–410.93	2.4570–3,489.000	419.6	39.70	0.1870	G	0	0	1.67	1.65	1.89	1.99	1.58	1.50
trans-2-Butene	46	195.20–363.15	1.1670–1,267.000	428.6	40.50	0.2140	G	-4.3160×10^{-2}	0	2.47	1.19	2.26	0.48	0.76	1.47
i-Butylene	37	216.41–410.93	8.7250–3,489.000	417.9	39.50	0.1900	G	0	0	1.42	1.41	1.54	1.31	1.24	1.14
cis-2-Butene	60	186.26–363.15	0.4946–1,180.000	435.6	41.50	0.2020	G	-1.2023×10^{-3}	0	1.80	1.76	1.60	2.88	2.58	1.86
1-Pentene	73	272.99–383.50	31.1600–863.400	464.7	34.80	0.2450	G	-9.4422×10^{-2}	0	3.45	0.59	3.40	3.37	3.68	3.35
1,3-Butadiene	78	197.60–413.15	1.9470–3,537.000	425.0	42.70	0.1950	G	1.7490×10^{-1}	−0.7224	2.21	1.84	2.26	1.47	1.65	1.47
Water	1,451	294.35–647.00	2.3960–22,100.000	647.3	214.75	0.3440	G	-4.2117×10^{-3}	−0.4499	10.47	1.04	11.20	8.05	10.58	10.35
Hydrogen	60	15.50–32.36	12.1600–1,136.000	33.2	12.80	−0.2200	G	-3.8608×10^{-2}	0	3.16	3.12	3.52	3.18	9.96	4.74
Neon	8	24.56–33.73	43.3400–510.200	44.4	27.20	−0.0414	G	3.8204×10^{-2}	0	3.80	3.43	4.03	6.76	7.97	5.35
Overall	**15,311**									**3.53**	**1.96**	**3.66**	**5.28**	**4.19**	**3.58**

*No good results could be obtained based on the generalized correlation of m_1.
G Generalized.

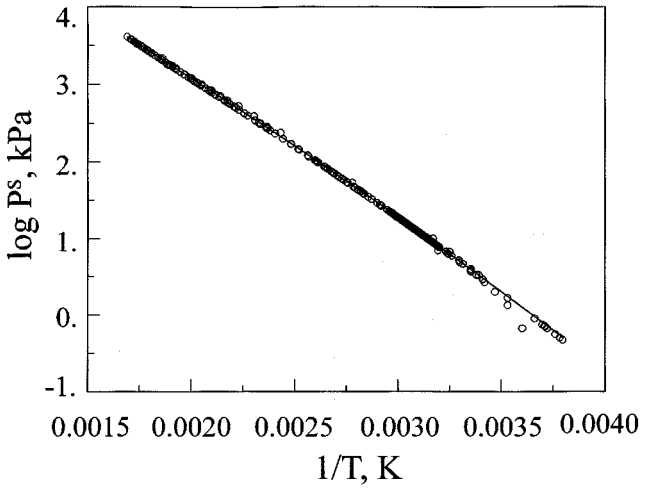

Figure 1. Calculated vs. experimental vapor pressure data of toluene.

The activity coefficients γ_i are calculated using the original UNIFAC model (Hansen et al., 1991). Figures 2 and 3 show the predicted results of the PSRK model for vapor-liquid equilibria of methane with different light alkanes and for the system methane-*n*-pentane at different temperatures. For the calculations, the pure component parameters from the generalized expressions (Eqs. 7 to 9) were used. As can be seen from the figures, the predicted results are in good agreement with the experimental data.

Prediction of VLE of Undefined Reservoir Oils and Natural Gases

Mixing rule of EOS parameters

Up to now, the PSRK group contribution mixing rule for the mixture parameters a and b of SRK EOS is limited to defined mixtures. For undefined petroleum mixtures, the following conventional mixing rules are used in this work

$$a = \Sigma\Sigma x_i x_j a_{ij} \tag{13}$$

$$a_{ij} = (a_i a_j)^{1/2}(1 - k_{ij}) \tag{14}$$

The parameter b required in Eq. 1 is calculated from Eq. 12.

Characterization of C7 + -fraction

A reservoir fluid mixture (oil or gas condensate) contains in addition to the defined light an undefined heavy hydrocarbons fraction (for example, the C7+-fraction). The properties of narrow cuts (pseudocomponents) are usually expressed in terms of average molecular weight and specific

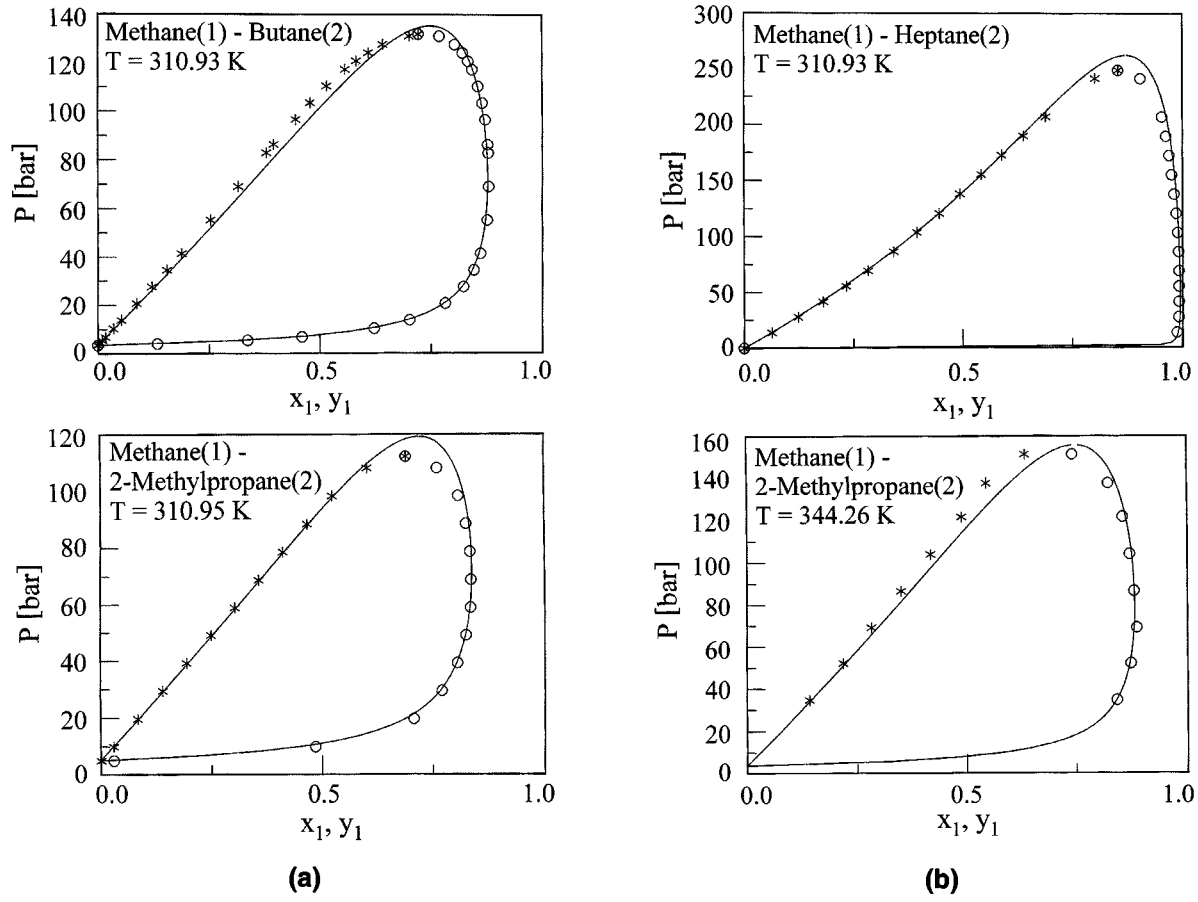

Figure 2. PSRK (UNIFAC) equation of state for vapor-liquid equilibria of methane with different light alkanes.

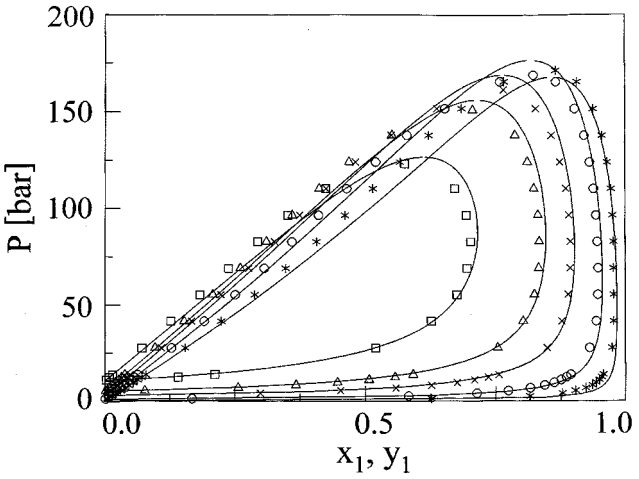

Figure 3. PSRK (UNIFAC) equation of state for vapor-liquid equilibria for the system methane-*n*-pentane at different temperatures.

∗ 277.59 K; ○ 310.93 K; × 344.26 K; △ 366.48 K; □ 399.82 K.

gravity (density of the liquid hydrocarbon relative to water at the same temperature). The required equation of state parameters for pure components are determined by the critical properties and the acentric factor, which are well defined for the light hydrocarbons but not readily available for the heavier hydrocarbon fractions. The characterization of C7-plus fractions involves the determination of the single carbon number (SCN) distribution, the division into pseudocomponents, the evaluation of the critical properties, and acentric factors of the pseudocomponents.

Determination of SCN distribution

(1) It is well known that, for naturally occurring hydrocarbon mixtures, a logarithmic relationship between the mole fraction x_N, and the corresponding carbon number (C_N) exists for $C_N > 7$. In the characterization methods proposed by Pedersen et al. (1984) a logarithmic distribution function of the mole fraction x_N of the SCN fraction vs. the carbon number C_N was assumed

$$C_N = A + B \ln x_N \tag{15}$$

where A and B are constants determined by a least-square fit to the experimental data of composition analysis for the lighter fractions. The results can be used to calculate the molar contents of the heavier fractions by extrapolation. However, if the measured value is not equal to the calculated one, A and B have to be changed to obtain agreement between the two quantities. In this case, the x_N value found for the heaviest fraction from the carbon number fractions is kept as the starting point for extrapolation. (The composition is known from the true boiling point (TBP) distillation process and gas chromatographic analysis.) The C_4 and C_5 fractions are analyzed for both normal and isoparaffins, while the C_6^+ fraction distilled off by a TBP distillation is split into carbon number fractions, that is C_6, C_7, and so on.

(2) The molecular-weight distribution of the plus fraction is determined by following equation (Guo and Du, 1989)

$$x_N = \frac{\sqrt{MW_N}}{A} \exp\left(\frac{-MW_N}{B}\right) \tag{16}$$

During the fitting of Eq. 15 or 16, the iteration stops when the molecular weight and the mole fraction of the plus fraction agree with the experimentally determined values. The composition and molecular weight of the individual components of the plus fraction can then be extrapolated on the basis of Eqs. 15 and 16 by satisfying the following mass balance

$$\sum_i x_i = x_p^+ \tag{17}$$

$$MW_p^+ = \sum_i x_i MW_i / x_p^+ \tag{18}$$

where the subscript p refers to the plus fraction and i refers to the individual component in the plus fraction. For compounds from C7 to C45 of the SCN fraction where experimental molecular weights are not available, the values suggested by Katz and Firoozabadi (1983) were used. For hydrocarbons with a carbon number greater than 45, the molecular weights were estimated using the following equation

$$MW_{CN} = -4.0 + 14.0\ C_N \tag{19}$$

(3) A fitting procedure can be established to determine the ''aromaticity'' of the plus fraction when the PNA distribution analysis data are not available. A logarithmic dependence of SG against carbon number is suggested on the basis of the work published by Pedersen et al. (1984)

$$SG(C_N) - SG(C_{N_0}) = D\left[\ln(C_N) - \ln(C_{N_0})\right] \tag{20}$$

D is a constant, $SG(C_N)$ is the specific gravity (such as relative density), and $MW(C_N)$ is the molecular weight of the carbon number fraction C_N. The starting point for the fitting procedure should be the specific gravity $SG(C_{N_0})$ of the heaviest carbon number fraction C_{N_0} for which a measured value is available. The extrapolated composition and molecular weight of the individual components in the plus fraction are used: the following objective function F must be very small (such as 10^{-8}) during the fitting procedure

$$F = \frac{\sum_i x_i MW_i}{SG_p^+} - \sum_i \frac{x_i MW_i}{SG_i} \tag{21}$$

In Eq. 21, the subscripts i and p are defined in the same way as in Eqs. 17 and 18. Finally, Eq. 20 is used to generate the SG values for the heavier fractions. With the method described above, the plus fraction of the sample can be split into single carbon fractions. Figures 4–6 show the split results for the C_i, M_i, and SG_i of the C_7^* fraction of oil sample 1.

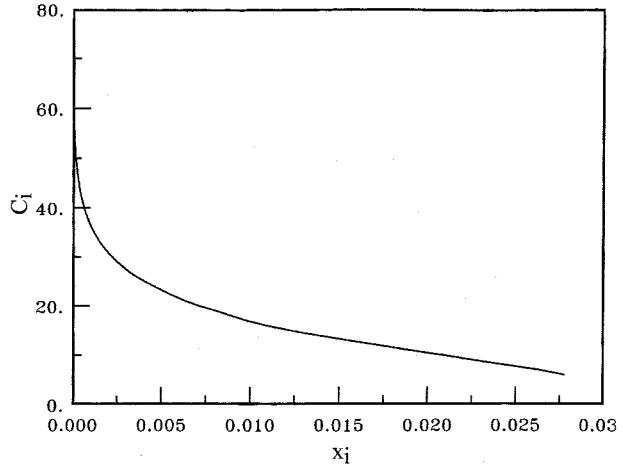

Figure 4. Split results of carbon number vs. mole fraction for the C7+ fraction of sample 1.

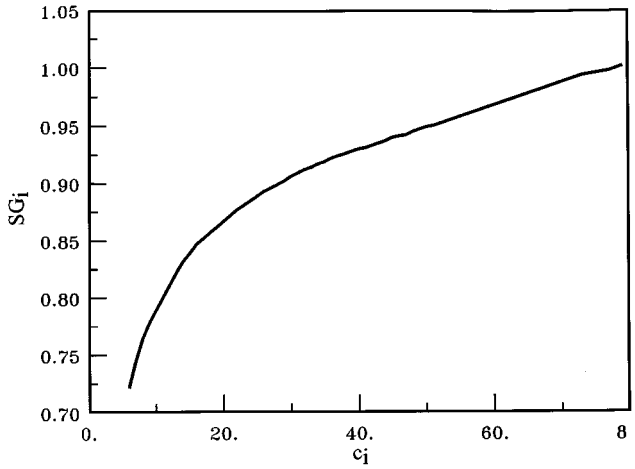

Figure 6. Split results of specific gravity vs. carbon number for the C7+ fraction of sample 1.

Lumping of the SCN fractions

The single carbon fractions were summed to give a certain number of pseudocomponents of approximately equal weight fraction. The average properties of the pseudocomponents were then calculated using the following mixing rule

$$x_{pc} = \sum_i x_i \tag{22}$$

$$MW_{pc} = \sum_i x_i MW_i \tag{23}$$

$$SG_{pc} = \frac{\sum_i x_i MW_i}{\sum_i x_i MW_i / SG_i} \tag{24}$$

where subscript i indicates the SCN fractions contained in the pseudocomponent. The above characterization procedure was used to separate the undefined C_7^+-fraction into three pseudocomponents with equal weight fractions.

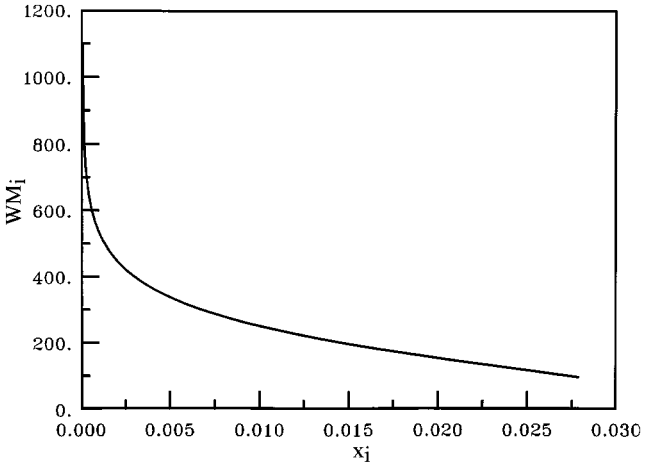

Figure 5. Molecular weight distribution for the C7+ fraction of sample 1.

Estimation of T_c, P_c and ω of pseudocomponents (pc)

The following empirical correlations are used for the SRK EOSs compared in this work:

(1) The normal boiling points T_b of the pseudocomponents are calculated by the Winn correlation (Pedersen et al., 1984)

$$T_{b\,pc} = \left(\frac{MW_{pc}}{5.805 \times 10^{-5}} SG_{pc}^{0.9371} \right)^{1/2.3776} \tag{25}$$

(2) The critical temperature T_c and the critical pressure P_c of the pseudocomponents are calculated from the correlations of Sim and Daubert (1980)

$$T_{C\,pc} = \exp\left(4.2009 \cdot T_{b\,pc}^{0.08615} \cdot SG_{pc}^{0.04614}\right)/1.8 \tag{26}$$

$$P_{C\,pc} = 6.1483 \times 10^7 \cdot T_{b\,pc}^{-2.3177} \cdot SG_{pc}^{2.4853} \tag{27}$$

(3) The acentric factor ω of the pseudocomponents is calculated using the correlation of Edmister (1958)

$$\omega_{pc} = \frac{3}{7} \frac{\log P_{C\,pc}}{\left(T_{C\,pc}/T_{b\,pc} - 1\right)} - 1 \tag{28}$$

where the values of T_b and T_c are given in K, those of SG are given in 15°C/15°C, and those of P_c are given in bar.

The SRK model combined with the above characterization methods can then be used to calculate the thermodynamic properties of complex undefined petroleum fluids.

Experimental data and calculated results

The sources of the oil and gas samples investigated in this article are listed in Table 2. The recombined wellstream composition and properties of plus fractions of these samples are given in Tables 6–8. The definition of rel. dev. (%) in this work can be obtained from an example of saturated pressure P^s as

$$\text{rel. dev. } (\%) = \left(P_{\text{cal}}^s - P_{\text{exp}}^s\right)/P_{\text{exp}}^s \times 100 \tag{29}$$

Table 2. Reservoir Crude Oils and Gas Samples

Sample No.	Oil* and Gas Source
1	Volatile crude oil, Fuyu oil field, China
2	Oil, No. 4 from Coats et al. (1986, see Du, 1991)
3	Oil, No. 7 from Coats et al. (1986, see Du, 1991)
4	North Sea oil
5	Oil, Lotsa Oil Co. PVT Report (1968)
7–9	CO_2 injected oils from Huabei oil field, China
10	Gas condensate from Yang et al. (1997)
11	Gas condensate from Ng et al. (1986)
12–15	Gas condensates from Wang and Guo (1990)
35–38**	Oils data collected by Du (1991)
39–43**	CO_2 injected oils from Jianghan oil field, China

*Oil data and the related measurement method were described by Du (1991).
**Original sample numbers used by Du (1991).

Table 4. Prediction of Bubble Point Pressure of CO_2-Injected Crude Oil Systems by SRK-2 Model

Sample No.	Temp. (K)	Exp. Bubble Pt. Pres. (MPa)	Rel. Dev. (%)
7	353.2	12.681	0.15
7	373.2	13.887	7.48
8	353.2	14.404	−1.83
8	373.2	16.093	4.01
9	353.2	17.196	−7.71
9	373.2	18.781	0.58
39	359.2	8.614	1.91
40	359.2	10.613	−4.27
41	359.2	12.095	1.40
42	359.2	13.818	1.27
43	359.2	22.440	−1.22
AAD, %			2.89

Bubble Point Pressure Prediction for Crude Oils. The experimental bubble point pressure data of the reservoir crude oils and a comparison with the results predicted using the SRK and SRK-2 models are listed in Table 3. It can be seen that in the case where $k_{ij} = 0$, both the SRK-2 and the original SRK models are able to predict lower bubble point pressures for most of the samples. However, SRK-2 provides better results than the original SRK model.

In Table 4 the experimental bubble point pressures and the predicted results for the CO_2-injected crude oil systems obtained from the SRK-2 model are listed. Very good accuracy is achieved when the SRK-2 model is combined with k_{ij} values from the following generalized correlations of k_{ij} developed for the original SRK EOS and crude oils (Du, 1991)

For methane (i)-hydrocarbon (j) systems

$$k_{ij} = \beta\left(\omega_j^{0.5} - \omega_i^{0.5}\right) \tag{30}$$

where $\beta = 0.07$ according to the results of Du for the original SRK EOS and $\beta = 0.033$ for the SRK-2 model in this work.

For carbon dioxide (i)-hydrocarbon (j) systems

$$k_{ij} = 0.12443 + 0.083828\,\omega_j - 0.093302\,\omega_j^2 \quad (\omega_j \le 0.35) \tag{31}$$

$$k_{ij} = 0.105 \quad (\omega > 0.35) \tag{32}$$

It should be mentioned that for such high CO_2 injections poor results are obtained for all the van der Waals types of EOS when k_{ij} is not used.

Dew Point Pressure Prediction for Natural Gases. Table 5 lists the experimental data and predicted results ($k_{ij} = 0$) for dew point pressures of the natural gas samples based on the improved and original SRK equations of state. From Table 5, it can be seen that both of the SRK equations of state predict lower dew point pressures when compared with the experimental values; however, better results are obtained for the SRK-2 model than for the original SRK equation of state.

The effect of tuning k_{ij} on the prediction results of the phase envelope of SRK EOS is shown in Figure 7. When a small k_{ij} value is used, the predicted dew point pressure can be increased. The predicted results of the SRK models for sample 11 with $k_{ij} = 0$ is shown by the dashed lines. When Eq. 30 is used with the coefficients 0.07 tuned to 0.033, the predicted results of SRK-2 are shown by a solid line. The results then agree perfectly with the experimental data.

Flash Calculation. The experimental VLE data of gas condensate (sample 11) by Ng et al. (1986) is used to check the results predicted by SRK-2. The measurement was carried out in a variable volume cell and the equilibrium phase properties were measured at 100°F (311 K) by expanding the volume of the equilibrium cell (reducing the pressure) from dew point (23 MPa) pressure. After the flash, the composi-

Table 3. Prediction of Bubble Point Pressure of Reservoir Crude Oil Systems

Sample No.	Temp. (K)	Exp. Bubble Pt. Pres. (MPa) ($k_{ij} = 0$)	Rel. Dev. (%) SRK-2	Rel. Dev. (%) SRK
1	338.2	17.37	−9.28	−13.85
1	348.2	17.99	−8.65	−12.83
1	360.2	18.68	−7.42	−11.78
2	316.5	13.60	−15.95	−19.14
3	328.2	11.78	−9.34	−15.46
4	360.4	22.94	5.52	−0.86
5	366.5	27.45	−25.88	−30.21
35	374.8	33.16	−1.15	−5.37
36	372.2	25.76	−8.43	−12.48
37	333.2	18.82	−5.42	−8.06
38	360.9	30.30	−8.35	−12.06
AAD, %			9.62	12.92

Table 5. Prediction of the Dew Point Pressure of Natural Gases with $k_{ij} = 0$

Sample No.	Temp. (K)	Exp. Dew Pt. Pres. (MPa)	Rel. Dev. (%) SRK-2	Rel. Dev. (%) SRK
10	390.5	46.07	−7.10	−12.99
10	410.1	45.31	−3.78	−9.72
10	429.5	44.66	−1.57	−7.92
10	450.3	42.88	2.25	−4.86
11	255.4	16.59	−12.08	−13.43
11	272.1	18.75	−6.90	−7.79
11	283.2	20.27	−6.10	−7.17
11	311.0	23.00	−4.62	−6.04
12	403.7	33.48	−2.25	−5.71
13	355.7	28.27	−3.90	−5.82
14	413.2	41.94	−24.14	−26.84
15	366.5	23.73	−8.13	−5.41
AAD, %			6.90	9.48

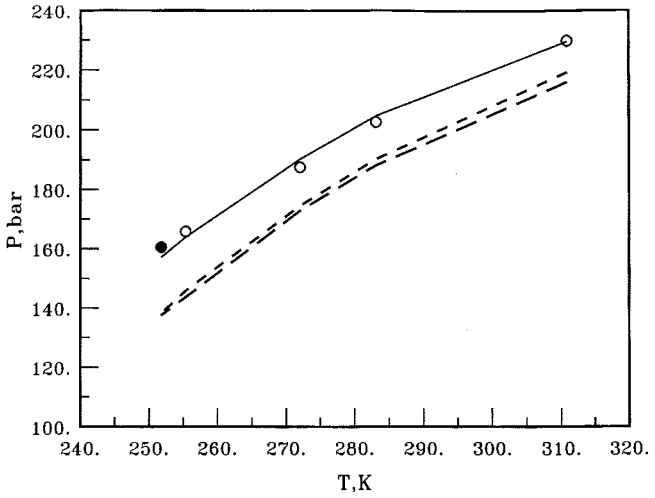

Figure 7. Calculated dew point line for a gas condensate using the SRK EOS and the effect of tuning k_{ij}.

● Experimental critical point; ○ experimental dew point (Yang et al., 1997); —— SRK ($k_{ij} = 0$); – – – SRK-2 ($k_{ij} = 0$); —— SRK-2 ($k_{ij} \neq 0$).

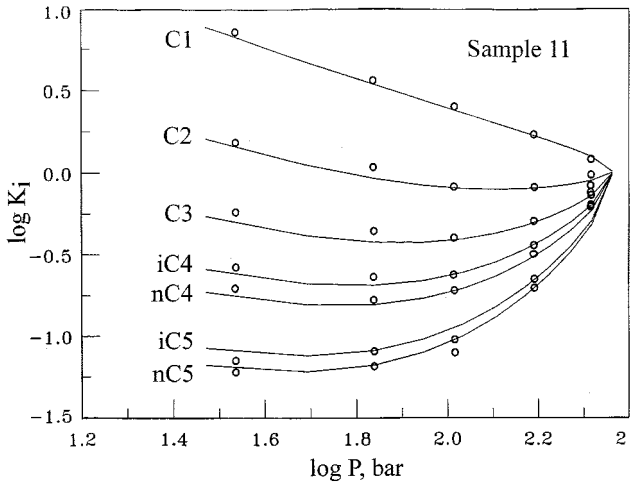

Figure 8. Equilibrium ratios using SRK-2 EOS for components in a gas condensate system at 311 K.

—— Predicted results; ○ experimental data: (Ng et al., 1986).

tions of the equilibrium phase were determined. The equilibrium ratios are given by

$$K_i = y_i/x_i \tag{33}$$

Figure 8 presents the experimental equilibrium ratios for the defined components in this gas condensate at 311 K and the simulation results for this experiment by the SRK-2 model, whereby the tuned coefficient 0.033 (Eq. 30) was used for the calculation. The agreement between the experimental data and the predicted results is satisfactory.

Conclusions

Based on a large number of vapor-pressure data taken from the Dortmund Data Bank (DDB), the parameters of the Mathias-Copeman α-function of the SRK EOS have been refitted for the components in petroleum fluids with a view to improving the accuracy of the vapor-pressure description at low pressures. Using the new parameters, the PSRK model is employed to calculate vapor-liquid equilibria for binary mixtures, the results being very satisfactory.

A characterization method has been applied for the SRK equation of state on the basis of existing empirical correlations for the properties of plus fractions of undefined mixtures. In most cases, where the PNA analysis data are not available, the molecular weight and specific gravity of the plus

Table 6. Composition of Reservoir Oil Samples and Properties of C7 + Fraction

	Sample No.								
Component	1	2	3	4	5	35	36	37	38
				Composition, mol. %					
CO_2	0.770	2.350	0.080	0.840	0.200	0.27	0.64	0.46	0.64
N_2	0.330	0.110	1.640	0.340	0.260	0.24		1.16	0.66
C1	40.874	35.210	28.400	49.230	47.630	66.83	52.39	41.86	58.80
C2	9.951	6.720	7.160	6.320	1.630	8.28	5.60	11.36	13.21
C3	8.351	6.240	10.480	4.460	1.180	5.15	6.31	9.60	7.36
*i*C4	2.840			0.860	0.610	1.04	2.31	1.18	0.88
*n*C4	3.580	5.070	8.400	2.180	0.640	2.27	3.12	5.12	3.21
*i*C5	1.420			0.930	0.450	1.00	1.66	1.27	0.83
*n*C5	1.070	5.230	3.820	1.330	0.410	1.04	1.66	0.22	1.48
C6	0.590	4.100	4.050	2.060	1.610	1.85	2.22	3.26	2.04
C7+	30.223	34.970	35.970	31.450	45.380	12.03	24.10		10.89
C7								2.53	
C8								3.47	
C9								2.76	
C10								2.13	
C11+								11.64	
				Properties of C7+-Fraction					
MW	213.0	213.0	252.0	230.3	224.0	182.0	199.0	261.0	188.0
SG	0.8179	0.8405	0.8429	0.8708	0.8478	0.801	0.822	0.8552	0.801

Table 7. Composition of CO_2 Injected Reservoir Oil Samples and Properties of C7+- Fraction

Component	Sample No. 7	8	9	39	40	41	42	43
				Composition, mol. %				
CO_2	41.631	46.435	51.521	12.642	21.656	33.195	40.917	61.685
N_2	0.276	0.253	0.229	0.145	0.130	0.111	0.098	0.064
C1	8.046	7.384	6.683	15.046	13.494	11.506	10.176	6.599
C2	2.477	2.273	2.057	5.156	4.624	3.943	3.487	2.261
C3	1.295	1.188	1.075	3.962	3.553	3.030	2.680	1.738
*i*C4	0.146	0.134	0.121	0.781	0.700	0.597	0.528	0.342
*n*C4	0.282	0.259	0.234	1.261	1.131	0.964	0.853	0.553
*i*C5	0.398	0.365	0.331	0.921	0.826	0.705	0.623	0.404
*n*C5	0.284	0.260	0.236	0.569	0.510	0.435	0.385	0.249
C6	1.610	0.931	0.718	0.180	0.162	0.138	0.122	0.079
C7+	44.447	40.789	36.916	59.334	53.212	45.375	40.130	26.024
				Properties of C7+-Fraction				
MW	295.0	295.0	295.0	282.0	282.0	282.0	282.0	282.0
SG	0.8785	0.8785	0.8785	0.8446	0.8446	0.8446	0.8446	0.8446

Table 8. Composition of Gas Condensate Samples and Properties of C7+- Fraction

Component	Sample No. 10	11	12	13	14	15
			Composition, mol. %			
CO_2	0.750		2.17	2.44	1.67	1.21
N_2	3.912		0.34	0.08	0.63	1.94
C1	70.203	74.133	70.64	82.10	78.51	65.99
C2	9.22	7.2086	10.76	5.78	8.86	8.69
C3	2.759	4.4999	4.94	2.87	3.21	5.91
*i*C4	0.662	0.8999	0.001	0.56	0.62	2.39
*n*C4	0.981	1.8088	3.019	1.23	0.95	2.78
*i*C5	0.402	0.8702	0.001	0.52	0.4	1.57
*n*C5	0.422	0.8889	1.349	0.60	0.35	1.12
C6	0.816	2.5925	0.9	0.72	0.46	1.81
C7+	9.873	7.0982*	5.88	3.10	4.34	6.59
			Properties of C7+-Fraction			
WM	192.8		153.0	132.0	149.0	140.0
SG	0.803		0.81	0.774	0.786	0.774

*Composition of C7+: C7, 3.1005; C8, 1.8631; C9,0.8364; C10, 0.6047; C11, 0.3296; C12, 0.1529; C13, 0.1012; C14, 0.0538; C15, 0.0208; C16, 0.0117; C17, 0.008; C18, 0.0065; C19, 0.0021; C20, 0.0014; C21, 0.0008; C22, 0.0007; C23, 0.0005; C24, 0.0004; C25, 0.0004; C26, 0.0003; C27+, 0.0003 mol. %

fraction can be employed to take into account the aromatic properties for the reservoir fluids by using the logarithmic distribution function of both the mole fraction and specific gravity of the SCN fraction vs. the carbon number of Pedersen et al. and the molecular-weight distribution function of Guo and Du. To estimate T_c, P_c, and ω of the pseudocomponents, the normal boiling points T_b are calculated by the Winn correlation, T_c and P_c are calculated from the correlations of Sim and Daubert, and ω is calculated from the correlation of Edmister.

The SRK equation of state together with the parameters of the Mathias-Copeman α-function fitted in this work has been used successfully for the calculation of the phase equilibrium behavior of undefined reservoir crude oils and natural gases. The calculated results show that the SRK models usually predict bubble or dew point pressures which are too low in the case where $k_{ij} = 0$. For SRK-2, better results are obtained when compared with the results of the original SRK model. Using a generalized correlation to predict k_{ij}, the accuracy of the VLE prediction can be improved for the reservoir crude oils, CO_2 injected crude oil, and natural gas systems. The calculations have been performed for very heavy reservoir crude oil samples (containing both high concentrations of methane and heavy fractions), CO_2 injected reservoir crude oil samples (containing high concentrations of CO_2, methane and heavy fractions), as well as gas condensate (in the vicinity of the critical point). That is so that it is clear that the α-expression is able not only to describe the phase equilibria for alkanes and aromatic hydrocarbons, but is also able to predict the thermodynamic properties for the very heavy components up to C_{80} which were not included when fitting the parameters. Therefore, the conclusion can be drawn that the SRK-2 model provides more reliable results for enhanced oil recovery and hydrocarbon processing than the original SRK model.

Acknowledgments

L.-S. Wang thanks the DAAD K.-C. Wong Foundation and National Nature Science Foundation of P.R. China for financial support and Dr. O. Noll and Mr. H. Gardeler for their help during his stay at the University of Oldenburg.

Notation

b = volumetric parameter of the SRK equation-of-state
C_i = carbon number of single carbon component i
k_{ij} = binary interaction parameter for parameter a
K_i = phase equilibrium ratio
m_i = parameter in the Mathias-Copeman expression
R = general gas constant
SG_i = specific gravity of single carbon component i
v = molar volume
x_i = mole fraction of component i in the liquid phase
y_i = mole fraction of component i in the vapor phase
M_i = molecular weight of single carbon component i, g/mol
α = temperature dependent function of the energy parameter a

Subscripts and Superscripts

calc = calculated value
exp = experimental data
M = mixture property
N_0 = heaviest fraction in the carbon number fractions
pc = pseudocomponent properties
r = reduced condition
s = saturated condition
$+$ = plus fraction

Literature Cited

American Petroleum Institute, ''Selected Values of Properties of Hydrocarbons and Related Compounds,'' Res. Project 44, 23-2: K, KA, KB, Amer. Pet. Inst. (1974).

Du, L.-G., ''Study on the High-Pressure Phase Behavior and Viscosity of Reservoir Crude Oil and CO_2-Injected Oil Systems,'' PhD Thesis, Univ. of Petroleum, Beijing (1991).

Edmister, W. C., ''Applied Hydrocarbon Thermodynamics: 4. Compressibility Factor and Equations of State,'' *Pet. Refiner*, **37**, 173 (1958).

Fischer, K., and J. Gmehling, ''Further Development, Status and Results of the PSRK Method for the Prediction of Vapor-Liquid Equilibria and Gas Solubilities,'' *Fluid Phase Equilib.*, **121**, 185 (1996).

Gmehling, J., *Dortmund Data Bank-Basis for the Development of Prediction Methods, CODATA Bulletin 58*, Pergamon Press, Oxford, U.K., p. 56 (1985).

Gmehling, J., ''Development of Thermodynamic Models with a View to the Synthesis and Design of Separation Processes,'' *Software Development in Chemistry: 5*, J. Gmehling, ed., Springer-Verlag, Berlin, p. 1 (1991).

Gmehling, J., J. Li, and K. Fischer, ''Further Development of the PSRK Model for the Prediction of Gas Solubilities and Vapor-Liquid Equilibria at Low and High Pressures: II, *Fluid Phase Equilib.*, **141**, 113 (1997).

Goodwin, R. D., ''Methanol Thermodynamic Properties from 176 to 673 K at Pressures to 700 bar,'' *J. Phys. Chem. Ref. Data*, **16**, 799 (1987).

Guo, T.-M., and L.-G. Du, ''A Three-Parameter Cubic Equation of State for Reservoir Fluids, *Fluid Phase Equilib.*, **52**, 47 (1989).

Hansen, H. K., P. Rasmussen, Aa. Fredenslund, M. Schiller, and J. Gmehling, ''Vapor-Liquid Equilibria by UNIFAC Group Contribution. 5. Revision and Extension,'' *Ind. Eng. Chem. Res.*, **30**, 2352 (1991).

Holderbaum, T., and J. Gmehling, ''PSRK: A Group Contribution Equation of State Based on UNIFAC,'' *Fluid Phase Equilib.*, **70**, 251 (1991).

Li, J., K. Fischer, and J. Gmehling, ''Prediction of Vapor-Liquid Equilibria for Asymmetric Systems at Low and High Pressures with PSRK Model,'' *Fluid Phase Equilib.*, **143**, 71 (1998).

Katz, D. L., and A. Firoozabadi, ''Boiling Points, Specific Gravities and Molecular Weight of Petroleum Fractions up to C_{45},'' *Pet. Technol.*, **20**, 1649 (1983).

Mathias, P. M., and T. W. Copeman, ''Extension of Peng-Robinson Equation of State to Complex Mixtures and Evaluation of Various Forms of Local Composition Concept,'' *Fluid Phase Equilib.*, **13**, 91 (1983).

Ng, H.-J., C.-J. Chen, and D. B. Robinson, ''Vapor Liquid Equilibrium and Condensing Curves in the Vicinity of the Critical Point for a Typical Gas Condensate (Project 815-A-84),'' Research Report RR-96, DB Robinson & Assoc. (1986).

Pedersen, K. S., P. Thomassen, and Aa. Fredenslund, ''Thermodynamics of Petroleum Mixtures Containing Heavy Hydrocarbons: 1. Phase Envelope Calculations by Use of the Soave-Redlich-Kwong Equation of State,'' *Ind. Eng. Chem. Process Des. Dev.*, **23**, 163 (1984).

Peng, D.-Y., and D. B. Robinson, ''A New Two-Constant Equation of State,'' *Ind. Eng. Chem. Fundam.*, **15**, 59 (1976).

Redlich, O., and J. N. S. Kwong, ''On the Thermodynamics of Solutions. V: An Equation of State. Fugacities of Gaseous Solutions,'' *Chem. Rev.*, **44**, 233 (1949).

Schmidt, G., and H. Wenzel, ''A Modified van der Waals Type Equation of State,'' *Chem. Eng. Sci.*, **35**, 1503 (1980).

Sim, W. J., and T. E. Daubert, ''Prediction of Vapor-Liquid Equilibria of Undefined Mixtures,'' *Ind. Eng. Chem. Process Des. Dev.*, **19**, 386 (1980).

Soave, G., ''Equilibrium Constants from a Modified Redlich-Kwong Equation of State,'' *Chem. Eng. Sci.*, **27**, 1197 (1972).

Soave, G., A. Bertucco, and M. Sponchiado, ''Avoiding the Use of Critical Constants in Cubic Equations of State,'' *AIChE J.*, **1**, 1964 (1995).

Wang, P., and T.-M. Guo, ''Regression of Experimental PvT Data for Gas Condensate Fluids,'' Research Report of University of Petroleum, Beijing (1990).

Yang, T., W.-D. Chen, and T.-M. Guo, ''Phase Behavior of a Near-Critical Reservoir Fluid Mixture,'' *Fluid Phase Equilib.*, **128**, 183 (1997).

Yu, J.-Min, and B. C.-Y. Lu, ''A Three-Parameter Cubic Equation of State for Asymmetric Mixture Density Calculations,'' *Fluid Phase Equilib.*, **34**, 1 (1987).

Manuscript received Oct. 1, 1997, and revision received Feb. 1, 1999.